Supporting Information

Designing a Self-Classifying Smart Device with Sensor, Display, and Radiative Cooling Functions via Spectrum-Selective Response

Sang Yeop Lee[a], Hangyu Lim[a], Jung Ho Bae[a], Dongwoo Chae[a], Taejong Paik[b], Heon Lee[a]* and Soong Ju Oh[a]*

Photoluminescence quantum yield of GCs

The photoluminescence quantum yield (PLQY) of GCs was analyzed via photoluminescence spectroscopy (Fig. S2). The GC PLQY is 80.53%, 83.99%, and 59.79% at an excitation wavelength of 300, 350, and 400 nm, respectively.

Optical properties of Cu-doped ZnS

The optical properties of Cu-doped ZnS were analyzed via UV-vis and PL spectroscopy (Figure S3 a, b). The UV-vis spectrum of Cu-doped ZnS shows that the absorption onset occurs at a wavelength of approximately 410 nm. The PL spectrum of Cu-doped ZnS exhibited a first peak at 448 nm and a second peak at 499 nm.

Transmittance of the 200-nm silver film

The transmittance of the 200-nm silver film was analyzed via UV-vis spectroscopy (Figure S5). The transmittance of the 200-nm silver film shows that no light is transmitted from 400 to 2500 nm. The absorption of the device from 400 to 2500 nm was calculated as follows:

$$R = 1 - A \qquad (1)$$

where R is the reflection and A is the absorption.

Principle of zero-energy radiative cooling

The law of energy conservation is the basic principle of zero-energy radiative cooling. The net cooling power of radiative cooling is defined as follows:

$$P_{Net\ cooling}(T) = P_{rad}(T) - P_{atm}(T_{amb}) - P_{sun} - P_{cond + conv} , \qquad (2)$$

where $P_{rad}(T)$ is the thermal radiation power, which in turn is defined as

$$P_{rad}(T) = A \int d\Omega \cos\theta \int d\lambda I_{BB}(T,\lambda)\varepsilon(\lambda,\theta) , \qquad \int d\Omega = 2\pi \int_0^{\pi/2} \sin\theta d\theta \qquad (3)$$

where A is the surface area of the sample, $\int d\Omega = 2\pi \int_0^{\pi/2} \sin\theta d\theta$ is the angular integral over the hemisphere $I_{BB}(T,\lambda) = \left(\frac{2h}{\lambda^5}\right)\left(e^{hc/\lambda k_B T} - 1\right)^{-1}$ is the specific intensity of the black body at temperature T, h is Planck's constant, c is the speed of light in a vacuum, λ is the wavelength, k_B is the Boltzmann constant, and $\varepsilon(\lambda,\theta)$ is the spectral and angular emissivity of the thermal radiation.

P_{atm} is the absorbed power by atmospheric radiation and is given by

$$P_{atm}(T_{amb}) = A \int d\Omega \cos\theta \int d\lambda I_{BB}(T_{amb},\lambda)\varepsilon(\lambda,\theta)\varepsilon_{atm}(\lambda,\theta) \qquad (4)$$

According to Kirchhoff's thermal radiation law, under thermodynamic equilibrium, the emissivity of the device is equal to its absorptivity.[1,2] The atmospheric emissivity is defined by $\varepsilon_{atm}(\lambda,\theta) = 1 - t(\lambda)^{\frac{1}{\cos\theta}}$, where $t(\lambda)$ is the atmospheric transmittance in the zenith direction.

P_{sun} is the power of the absorbed solar radiation and is expressed as follows:

$$P_{sun} = A \int_0^\infty d\lambda \varepsilon(\lambda,\theta_{sun}) I_{AM1.5}(\lambda) , \qquad (5)$$

where $I_{AM1.5}$ is the illumination intensity of the solar radiation.

The conduction and convection power is defined as follows:

$$P_{cond + conv}(T,T_{amb}) = Ah_c(T_{amb} - T) , \qquad (6)$$

where h_c is the non-radiative transfer mechanism coefficient.[3,4]

Zero-energy radiative cooling performance

A radiative cooling device was fabricated as follows (Figure S9a). A 200-nm layer of silver was deposited on the glass substrate using a thermal evaporator. The PDMS was spin-coated onto the silver layer at 1000 rpm for 30 s. Outdoor measurements were conducted to measure the cooling performance of the radiative cooling device using the same chamber and on the same day as the smart device measurements. The radiative cooling device was cooled by 14.8 °C during the daytime and by 10.6 °C at night (Figure S9b).

Cooling performance of the smart device

The environmental factors that can affect the radiative cooling performance were measured (Figure S10a, b, and c). To verify the radiative cooling performance of the smart device, the cooling temperature and cooling power were simulated using the equations of the principle of zero-energy radiative cooling based on weather data measured on the same day. The heat-transfer coefficient was set to 3.5.[5] The cooling power of the PET–Ag–PDMS–ITO PET radiative cooling device at the ambient temperature (278 K) and a solar power of 500 W m^{-2} was 53.9 W m^{-2} and the cooling power of the smart device was 43.5 W m^{-2} (Figure S11a). The cooling temperatures of the devices were 7.4 and 6.0 °C, respectively, under the same conditions (Figure S11b). The cooling power of the devices were 58.1 and 47.7 W m^{-2}, respectively, at an ambient temperature of 300 K and solar power of 550 W m^{-2} (Figure S11c). The cooling temperatures of the devices were 7.9 and 6.5 °C, respectively, under the same conditions (Figure S11d). Based on the simulated cooling power, temperature, and measured ambient temperature, the expected cooling temperature during the day on November 27, 2021, was simulated (Figure S12). The simulated cooling temperatures showed good agreement with the outdoor measurement results and exhibited a similar trend.

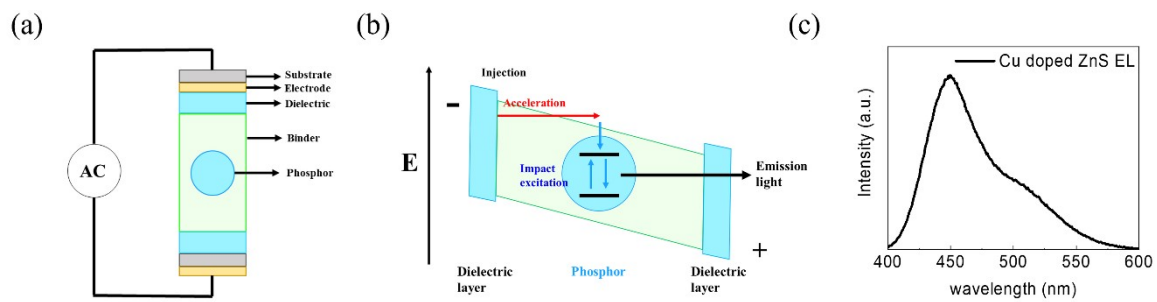## Supplementary Figures

(a)

(b)

(c)

Figure S1. (a) Schematic of the electroluminescence device. (b) Light-emitting mechanism of the electroluminescence device. (c) EL spectrum of Cu-doped ZnS.
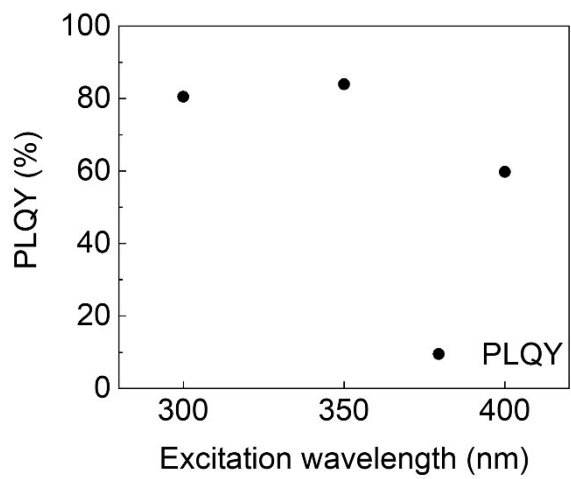
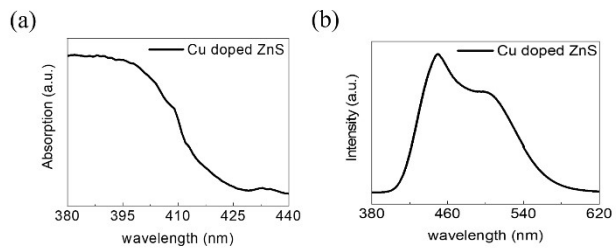Figure S2. Photoluminescence quantum yield of the GC

(a)

(b)

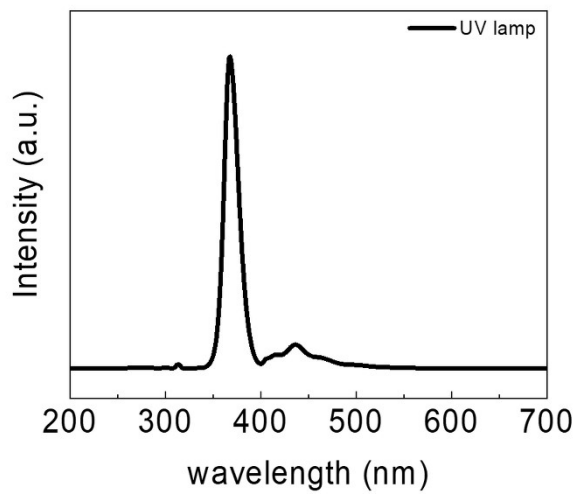Figure S3. (a) UV-vis and (b) PL spectra of Cu-doped ZnS.
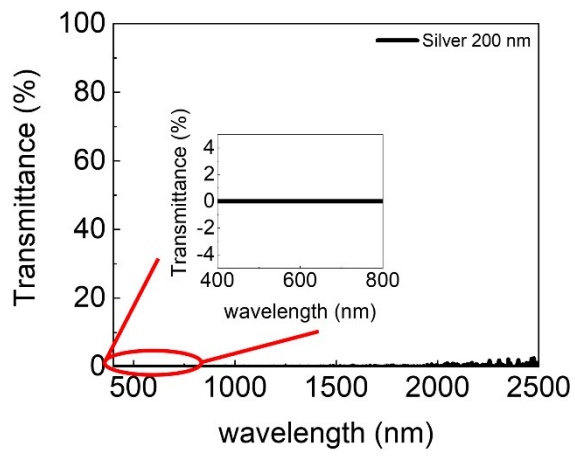
Figure S4. 365-nm UV lamp spectrum
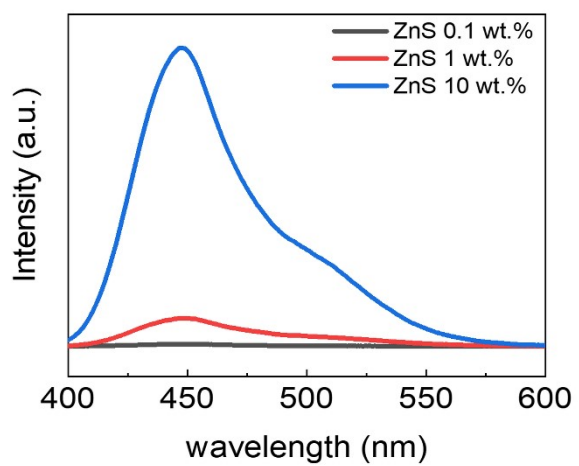
Figure S5. Transmittance of the 200-nm silver film

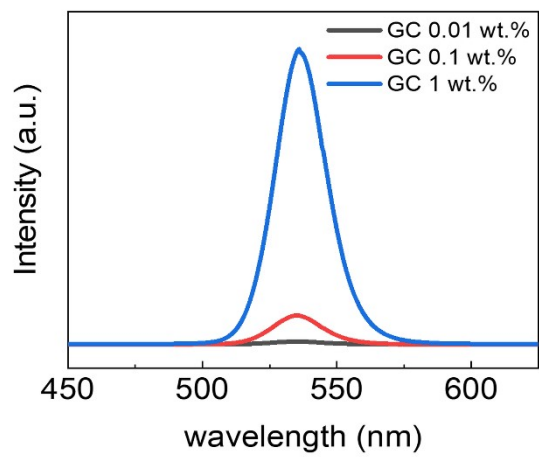Figure S6. EL spectra of Cu-doped ZnS with different weight ratios

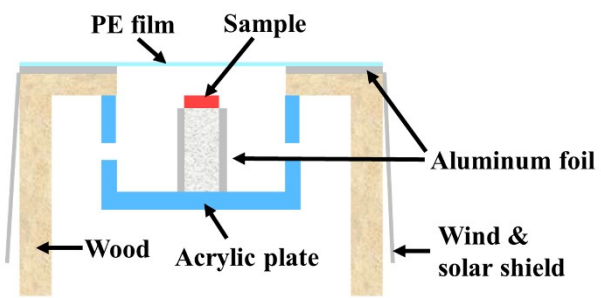Figure S7. PL spectra of GCs with different weight ratios

Figure S8. Schematic of the chamber used for the outdoor measurements
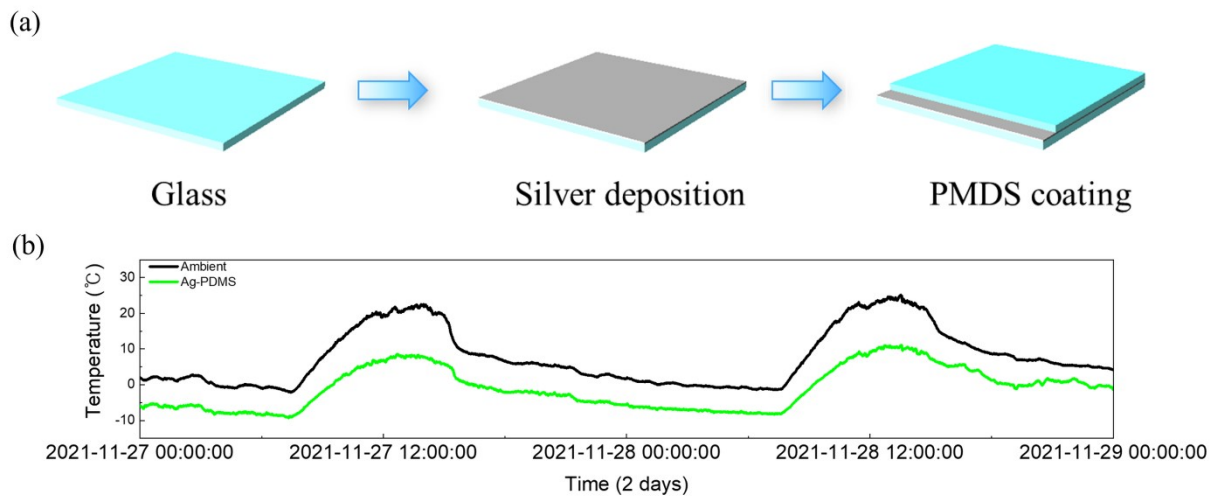
(a)

Glass → Silver deposition → PMDS coating

(b)

Figure S9. (a) Fabrication of the radiative cooling device. (b) Outdoor measurements of the Ag-PDMS radiative cooling device on November 27 and 28, 2021.
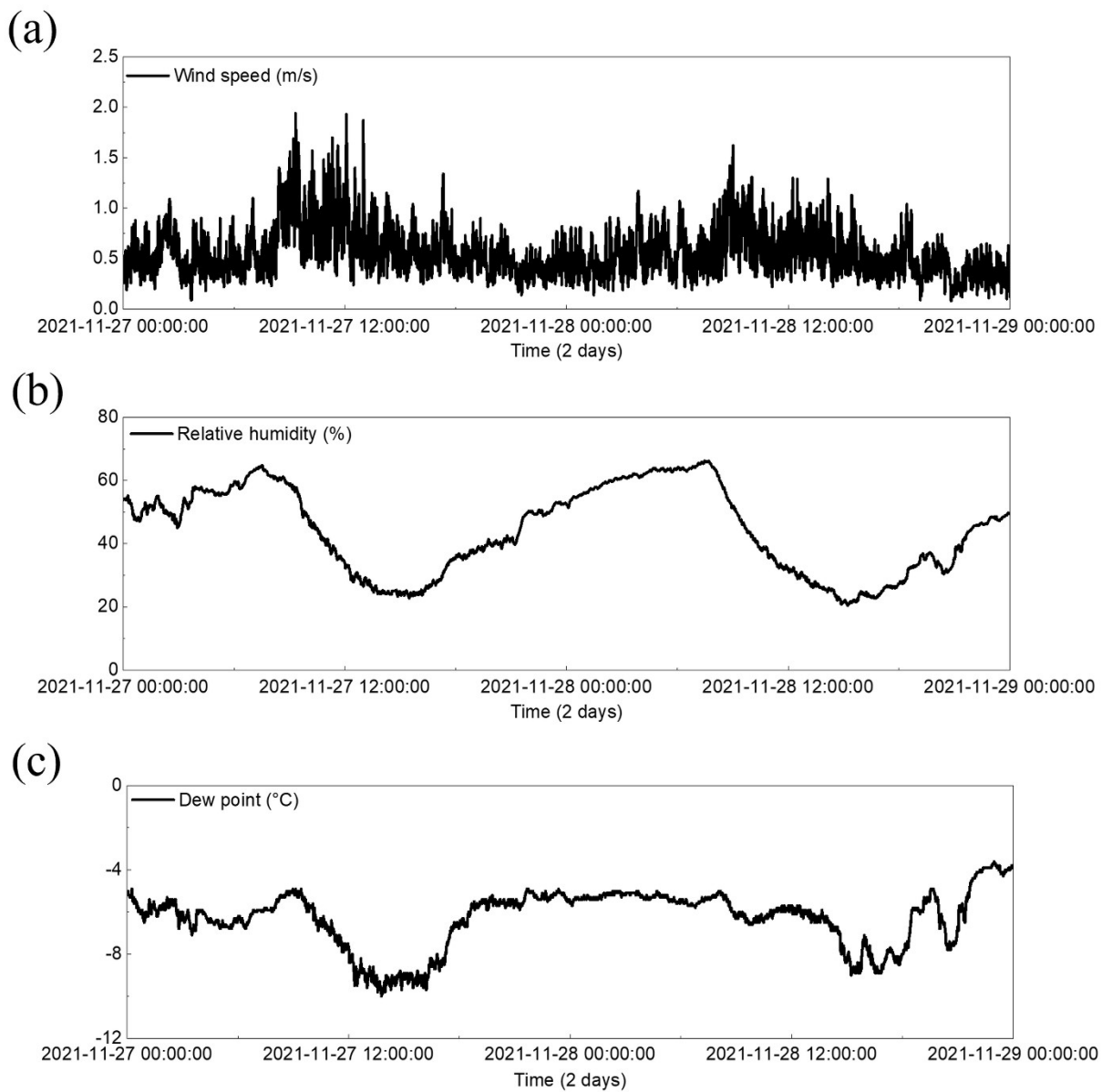
Figure S10. (a) Wind speed, (b) relative humidity, and (c) dew point on November 27 and 28, 2021.
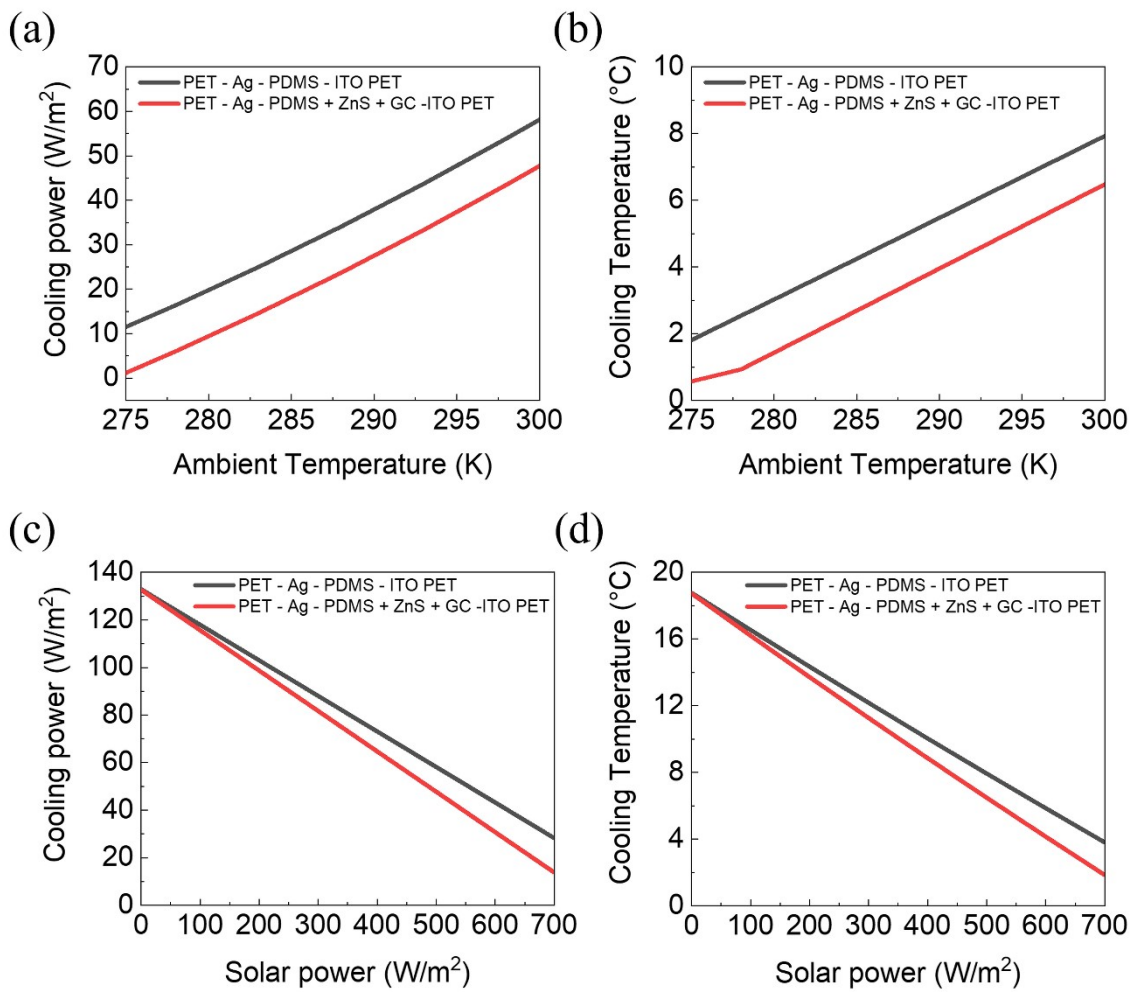
Figure S11. Simulation of (a) cooling power as a function of ambient temperature, (b) cooling temperature as a function of ambient temperature at a solar power of 500 W m^{-2}, (c) cooling power as a function of solar power, and (d) cooling temperature as a function of solar power at an ambient temperature of 300 K.
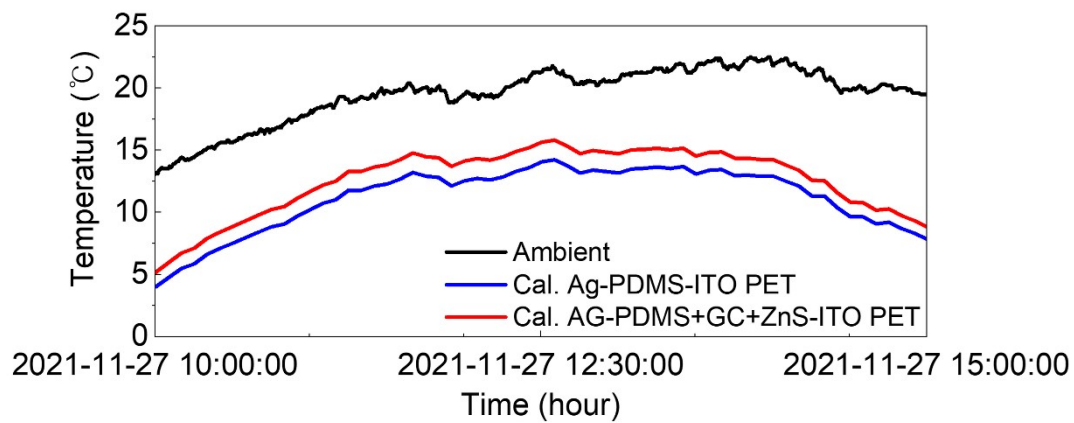
Figure S12. Simulation of cooling temperature on November 27, 2021, during daytime
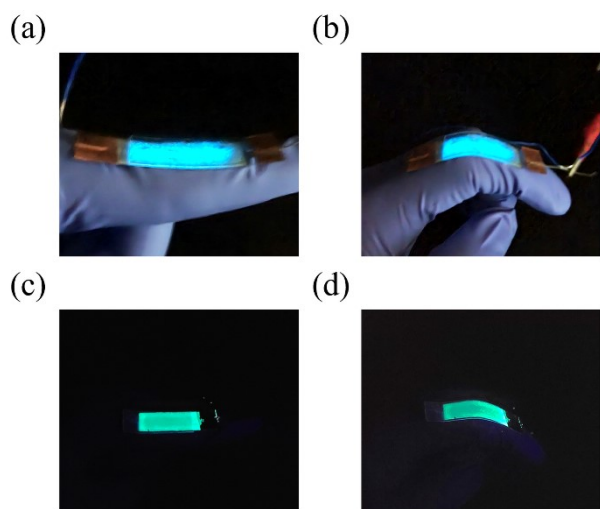
(a)　　　　　　　　(b)

(c)　　　　　　　　(d)

Figure S13. (a) Image of the device attached to a human finger with blue EL light. (b) Image of the device with blue EL light after bending the finger. (c) Image of the device attached to the finger with green PL light. (d) Image of the device with green PL light after bending the finger.

References

1   Y. Nishijima, A. Balčytis, S. Naganuma, G. Seniutinas and S. Juodkazis, *Sci. Rep.*, **2019**, *9*, 1–9.

2   A. P. Raman, M. A. Anoma, L. Zhu, E. Rephaeli and S. Fan, *Nature*, **2014**, *515*, 540–544.

3   S. Jeon, S. Son, S. Y. Lee, D. Chae, J. H. Bae, H. Lee and S. J. Oh, *ACS Appl. Mater. Interfaces*, **2020**, *12*, 54763–54772.

4   S. Park, J. Bang, B. S. Kim, S. J. Oh and J. H. Choi, *Mater. Today Adv.*, **2021**, *12*, 0–6.

5   J. Liu, J. Zhang, D. Zhang, S. Jiao, J. Xing, H. Tang, Y. Zhang, S. Li, Z. Zhou and J. Zuo, *Renew. Sustain. Energy Rev.*, **2020**, *130*, 109935.